Proceedings of 20th International Congress on Acoustics, ICA 2010

23-27 August 2010, Sydney, Australia

Measurement and Modelling of Underwater Noise from Pile Driving

Alec J Duncan, Robert D McCauley, Iain Parnum and Chandra Salgado-Kent

Centre for Marine Science and Technology, Curtin University, Perth, Western Australia

PACS: 43.30Zk, 43.50Pn, 43.80Nd.

ABSTRACT

Many coastal and offshore construction activities require the driving of piles into the seabed, either using impact or vibratory pile drivers. Impact pile driving produces an intense impulsive underwater noise that has been associated with fish deaths at very short range, whereas vibratory pile driving produces a lower level continuous noise. Because of the high sound levels involved, noise from pile driving may have an adverse impact on marine animals, and its characteristics are therefore of considerable interest. This paper presents the results of measurements of underwater noise from pile driving that have been made at a variety of locations around Australia, and presents the results of some attempts to use acoustic propagation modelling to extrapolate these results to other locations.

INTRODUCTION

Impact pile driving, a common aspect of coastal and offshore construction, is known to produce loud, impulsive underwater sounds that are potentially detrimental to marine life (David, 2006, Popper and Hastings, 2009). Lethal effects on fish have been reported at short ranges (less than a few metres), and at longer ranges there is the possibility of damage to hearing organs and adverse behavioural impacts. Because of this, government regulators now often require predictions of underwater noise from pile driving and a consideration of its possible environmental effects as part of environmental impact statements from companies planning coastal or offshore construction projects.

Predicting underwater noise from pile driving is complicated by the nature of the sound source and by the strong interaction that occurs in shallow water between sound waves in the water and various types of waves travelling in the seabed and along the water-seabed interface.

When the pile is struck by a hammer, underwater sound can be produced by a number of mechanisms:

- Direct radiation of sound into the water by the portion of the vibrating pile that is in the water column.
- Mechanical vibrations and the sudden displacement of the portion of the pile in the seabed, resulting in the radiation of both shear and compressional waves in the seabed that can reach the seafloor by a variety of paths and subsequently couple back into sound waves in the water.
- The motion and vibration of the pile generates surface (Scholte) waves that propagate along the water/seabed interface but also produce pressure fluctuations in the water column that are particularly significant close to the seabed.

There is no currently available numerical software that can adequately model the complexities of this process from first principles for realistic scenarios. This paper therefore presents an alternative approach that uses an equivalent point source model combined with a numerical acoustic propagation code to extrapolate pile driving noise measurements made at one location to a different location. This method is certainly not perfect and more validation is required, however initial comparisons with field data are encouraging.

MEASURED PILEDRIVING NOISE

The Centre for Marine Science and Technology has carried out a number of measurements of pile driving noise in Port Phillip Bay, Victoria, Australia for the Port of Melbourne Corporation. Two of these data sets were selected for further analysis on the basis that the types of piles and the parameters of the equipment driving the piles were well known, and the measurements were made under favourable conditions, leading to good signal to noise ratio over a wide range of frequencies. The data sets were from different locations with quite different seabed properties (see Figure 1). Gellibrand Wharf is at the northern end of Port Phillip Bay, close to where the Yarra River discharges and the seabed at this location comprises a thick layer of fine silt over sand (Holdgate et. al., 2001). South Channel is at the southern end of the bay where there is considerable tidal scour and the seabed consists of a layer of coarse sand overlying calcarenite, a weakly cemented limestone.

Table 1 provides a summary of the measurement scenarios for the two sets of field data, and the piles and pile driving equipment used in each case. The same types of piles were used in both cases, but the pile driving equipment was different.

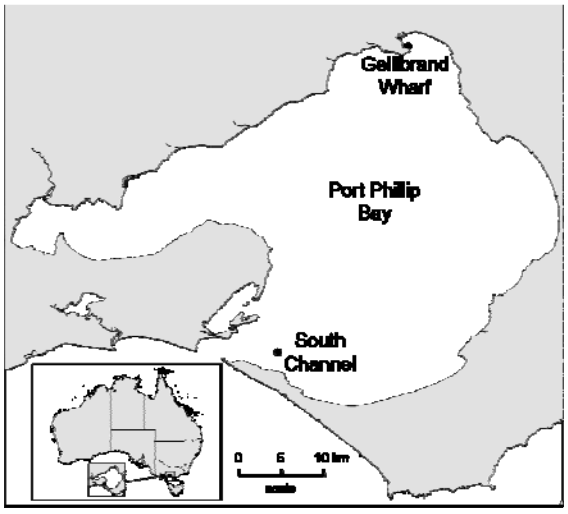

Figure 1. Locations of measurement sites at Gellibrand Wharf and South Channel.

Table 1. Measurement and source parameters for the two data sets

Measurement location	Gellibrand Wharf (37° 51.8'S, 144° 54.9'E)	South Channel (38° 18.0'S, 144° 43.9'E)
Water depth(s)	8.5m to 12.6m (see Figure 2)	13m
Hydrophone depth	4m	4m
Pile descriptions	Steel, 711mm OD, 21 mm wall	Steel, 711mm OD, 21 mm wall
Hammer description	IHC S90 hydro hammer	KV Johnson Marine custom 5 tonne hammer with 1.2 m stroke.
Hammer energy	2 kN.m to 90 kN.m	59 kN.m
Span of measurement ranges analysed	38 m to 260 m	71 m to 457 m

The seabed at the South Channel site was flat, whereas the seabed profile at Gellibrand Wharf was complicated by the dredged berth. In the latter case, measurements were made along several different azimuths. In the absence of measured bathymetry profiles the approximate profile shown in Figure 2 was obtained from the hydrographic chart of the area. The same profile was used for all azimuths because the charted bathymetry was not considered accurate enough to warrant the added complexity of using a different profile for each acoustic path.

In both cases recordings were made using a single factory calibrated Reson TC4033 hydrophone at 4m depth, a Reson VP1000 preamplifier, and a Sound Devices 744T digital recorder set to 48 kHz sample rate and 24 bit resolution.

System gain was calibrated by replacing the hydrophone with a white noise generator that outputs white noise of known spectral density. The noise output by the generator has a flat spectrum from 10 Hz to the upper frequency limit of the recording instrumentation. The system gain response, the hydrophone sensitivity, the recording gain settings and the SD744T normalisation gain (±5.5 V to ±1 V) were used to convert the recorded signal to Pa.

Distances between the pile and hydrophone were measured in the field whenever possible using Bushnell laser range finding binoculars targeted on the pile. GPS locations of the receiver and pile were used as a backup.

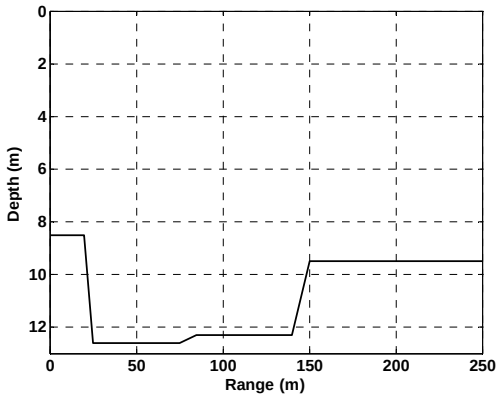

Figure 2. Bathymetry used for Gellibrand Wharf pile driving source analysis

Analysis of the recorded data included calculation of peak to peak, mean square and sound exposure (integrated squared pressure with estimated ambient noise subtracted) levels for each recorded impact. Mean square levels were calculated over the signal duration, which was defined as the time interval containing 90% of the received energy. Mean square and sound exposure levels are related by:

$$L_{SEL} = L_{ms} + 10\log_{10}(T) \quad (1)$$

where L_{SEL} is the sound exposure level (dB re 1 μPa^2.s), L_{ms} is the mean square level (dB re 1 μPa^2), and T is the signal duration in seconds. L_{SEL} and L_{ms} are therefore numerically equal when the signal duration is one second.

In Figure 3, peak to peak levels are plotted as a function of range for both data sets. Sound exposure levels (SELs) are plotted against range in Figure 4. Both plots show a faster reduction in level with range at Gellibrand Wharf than at South Channel, which is a result of the softer, more absorptive seabed at the northern end of the bay.

A scatter plot of peak to peak level against SEL is given in Figure 5. All measured impacts from both sites are within +/- 3 dB of the regression line:

$$L_{p-p} = 1.12L_{SEL} + 12.3 \quad (2)$$

Where L_{p-p} is the peak to peak level (dB re 1μPa p-p) and L_{SEL} is the sound exposure level (dB re 1 μPa^2.s).

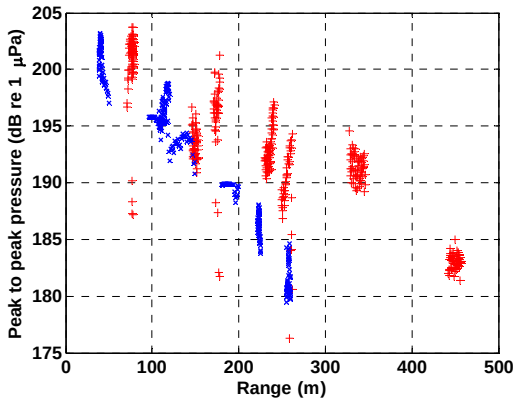

Figure 3. Peak to peak level (dB re 1 µPa p-p) vs range for all recorded impacts. Blue x: Gellibrand Wharf, red +: South Channel.

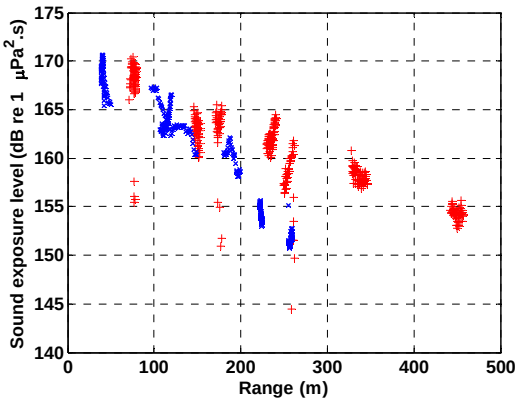

Figure 4. Sound exposure level (dB re 1 µPa^2.s) vs range for all recorded impacts. Blue x: Gellibrand Wharf, red +: South Channel.

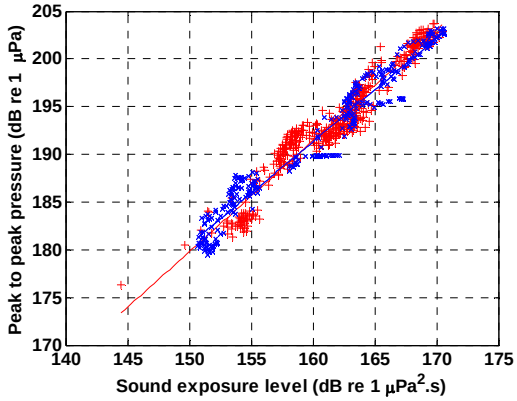

Figure 5. Scatter plot of peak to peak level vs SEL for all recorded impacts. Blue x: Gellibrand Wharf, red +: South Channel. Red line is $L_{p-p} = 1.12L_{SEL} + 12.3$.

A scatter plot of mean square level against SEL is shown in Figure 6. In this case the line of best fit is:

$$L_{ms} = 1.23L_{SEL} - 23.9 \quad (3)$$

where L_{ms} is the mean square level (dB re 1 µPa^2) . There are, however, a number of outliers which is a reflection of the sensitivity of the mean square level measurements to the determination of the signal length, which is intrinsically variable depending on the multipath structure reaching the receiver.

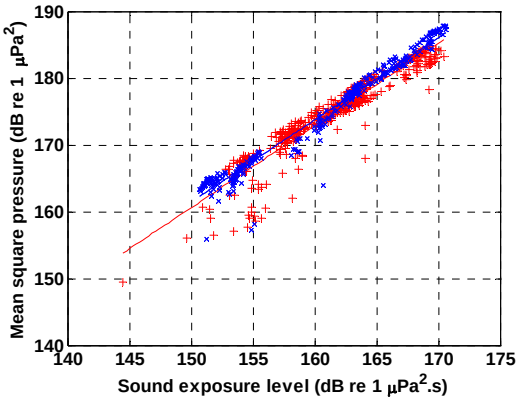

Figure 6 Scatter plot of mean square level vs SEL for all recorded impacts. Blue x: Gellibrand Wharf, red +: South Channel. Red line is Mean square level = 1.23 x SEL -23.9.

EXTRAPOLATION OF MEASUREMENTS TO OTHER LOCATIONS

The approach taken to extrapolating the measured data to other locations was to assume that the complicated radiation from the pile could be replaced by an equivalent point source located on the seabed at the base of the pile. The source spectrum of this equivalent point source was derived from measured data and then combined with transmission loss calculations from another site to predict likely received levels as a function of range at the new site.

Estimation of source spectrum

The source spectrum of this equivalent point source was obtained by the following procedure:

- A numerical acoustic propagation model was used to compute transmission loss as a function of range at one-twenty-fourth octave intervals from 20 Hz to 14254 Hz.
- An average transmission loss curve was calculated for each one-third octave band by averaging the transmission loss curves within the band. This was done by converting each transmission loss curve to equivalent received pressure, squaring, averaging, and then converting back to transmission loss.
- For each measurement range, the measured sound exposure level (SEL) in each one-third octave frequency band was calculated by integrating the energy density spectrum of the received signal over the required frequency band. This process was carried out using the re-

corded impact with the highest overall SEL at each range so that the results corresponded to the worst-case source level.

- The measured SEL in each one-third octave band was combined with the average modelled transmission loss to obtain an estimate of the source level in that band.
- The source levels computed using signals received at different ranges were then averaged in the dB domain to obtain the final source level estimate for each frequency band.

The above process was carried out for the two measured data sets using the acoustic propagation models and seabed parameters listed in Table 2. RAMGeo is a parabolic equation model suitable for propagation over range-dependent fluid seabeds whereas SCOOTER is a wavenumber integration code suitable for range-independent elastic seabeds. Further details of these codes can be found at http://oalib.hlsresearch.com/. The physical principles of these methods are described in Jensen et. al. (2000).

Table 2. Acoustic propagation modelling codes and seabed geoacoustic parameters used for source level estimates.

	Gellibrand Wharf	**South Channel**
Propagation model	RAMGeo, layered fluid seabed with range dependent bathymetry	SCOOTER, range independent fluid/elastic seabed
Seabed geoacoustic model	*Water column*: variable depth (see Fig 1), c_p = 1500 m/s, ρ = 1024 kg.m^{-3} *Silt layer*: 4m thick, c_p = 1575 m/s, ρ = 1700 kg.m^{-3}, α_p = 1.0 dB/λ *Fine sand layer*: 14m thick, c_p = 1650 m/s, ρ = 1900 kg.m^{-3}, α_p = 0.8 dB/λ *Coarse sand halfspace*: c_p = 1750 m/s, ρ = 1950 kg.m^{-3}, α_p = 0.6 dB/λ	*Water column*: 13 m deep, c_p = 1500 m/s, ρ = 1024 kg.m^{-3} *Coarse sand layer*: 6m thick, c_p = 1750 m/s, ρ = 1950 kg.m^{-3}, α_p = 0.6 dB/λ *Calcarenite halfspace*: c_p = 2400 m/s, ρ = 2400 kg.m^{-3}, α_p = 0.1 dB/λ, c_s = 1000 m/s, α_s = 0.2 dB/λ

The seabed geoacoustic parameters were arrived at by a combination of consideration of the geology described in Holdgate et. al. (2001), and some trial and error to match the measured and predicted rates of decay of received level with range in each one-third octave band. The main change required to obtain a reasonable match for frequencies below 100 Hz was to include deeper, higher speed layers in the geological models.

The source spectra obtained from the two sets of data are shown in Figure 7 and are very similar for frequencies above 100 Hz, but differ significantly at lower frequencies. It is unknown whether the high source level values at low frequencies are real or are due to the sensitivity of acoustic propagation in this frequency range to the poorly known sub bottom layering, combined with the naturally high levels of low frequency ambient noise.

Combining the source spectra over frequency gave the broadband source SELs listed in Table 3.

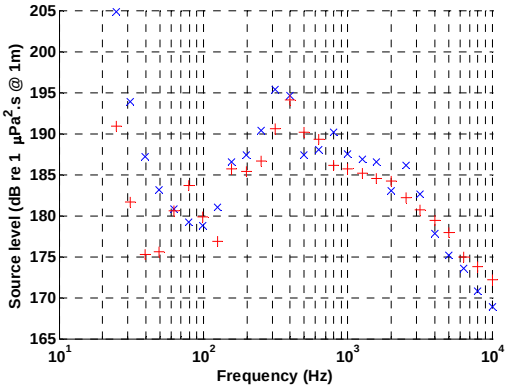

Figure 7. Estimated source sound exposure level in each 1/3 octave band. Blue x, Gellibrand wharf; red +, South Channel.

Table 3. Broadband source sound exposure levels for different frequency ranges

Frequency range	25 Hz to 12 kHz	100 Hz to 12 kHz
Gellibrand Wharf	205.3 dB re 1 µPa^2.s @ 1m	201.2 dB re 1 µPa^2.s @ 1m
South Channel	200.2 dB re 1 µPa^2.s @ 1m	199.6 dB re 1 µPa^2.s @ 1m

Prediction of received levels

Prediction of received levels in a new location can be carried out by using an appropriate acoustic propagation code to compute the transmission loss at different frequencies for the new scenario, and then combining these with the source spectrum to obtain the received levels.

An assumption inherent in this procedure is that the source spectrum is the same in the new scenario as it was in the situation where it was originally measured. There are a number of reasons why this may not be the case, for example changes to pile types or sizes, different pile-driving equipment, different water depth, and different seabed composition at the piling site, particularly the hardness of the shallow substrate. However, when similar piles are being driven by similar equipment and the seabeds don't differ too much there is some justification in using this approach.

As a test, this method was applied to the Gellibrand Wharf and South Channel data, but with the source spectrum measured at Gellibrand Wharf used to predict the South Channel received levels and vice-versa. Once again transmission loss calculations were done using RAMGeo (Gellibrand Wharf) and SCOOTER (South Channel). Transmission loss was

calculated at one-twenty-fourth octave frequencies from 20 Hz to 14254 Hz and averaged over one-third octaves.

Results are plotted in Figure 8 and Figure 9, and Table 4 lists the root mean square (rms) and mean dB differences between the predicted and measured sound exposure levels. As a comparison, the table also shows the rms and mean differences between the measured received levels and those predicted using the source spectrum measured at the same site. Note that both the predicted and measured levels given in these results are for the maximum sound exposure level at each range.

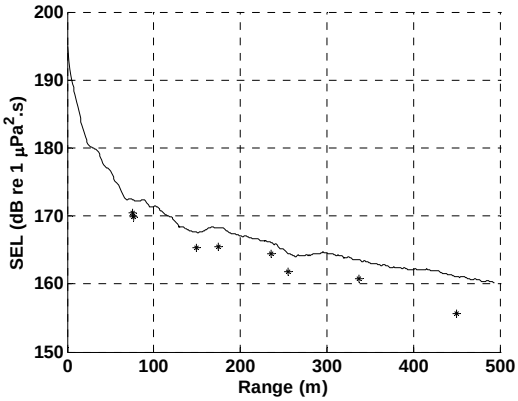

Figure 8. Line is predicted South Channel maximum received SEL derived using source spectrum obtained from Gellibrand Wharf data. Points are measured maximum SELs from South Channel.

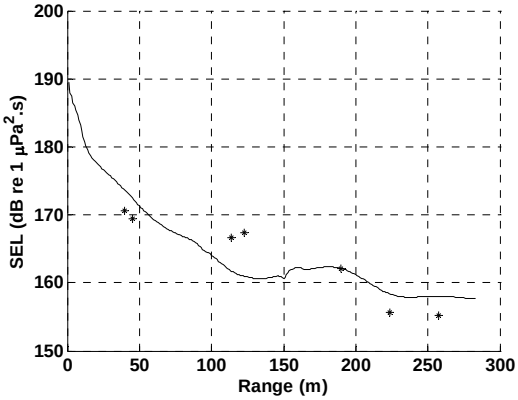

Figure 9. Line is predicted Gellibrand Wharf maximum received SEL derived using source spectrum obtained from South Channel data. Points are measured maximum SELs from South Channel.

Interestingly, these results indicate that using the South Channel source spectrum to predict the Gellibrand Wharf data results in a slightly better fit to the data than using the Gellibrand Wharf spectrum. This may, however, be somewhat misleading as the comparison here is between sound exposure levels integrated across the entire spectrum, whereas the source spectra were estimated by minimising the differences between predicted and measured received spectra.

Table 4. Root mean square difference between predicted and measured maximum SELs (dB). Mean difference is in brackets.

		Source Spectrum	
		Gellibrand Wharf	South Channel
Measured data	Gellibrand Wharf	4.2 (1.5)	3.7 (0.1)
	South Channel	3.0 (2.7)	1.2 (0.7)

CONCLUSIONS

Underwater acoustic source spectra obtained for two 711mm diameter steel piles being driven at two widely separated locations in Port Phillip Bay with quite different seabeds were very similar for frequencies above 100 Hz and peaked between 300 Hz and 400 Hz. There were greater discrepancies between the measured spectra at lower frequencies but it is unclear whether these differences are real or an artefact of the method used to estimate the source spectrum.

Both data sets show a linear relationship between peak to peak level and sound exposure level with all data points falling within +/- 3 dB of the line defined by Equation (2). A similar linear relationship, albeit with more outliers, was found between mean square level and sound exposure level.

Despite the differences in pile driving equipment and seabeds at the two sites, when the source spectrum measured at one site was used to predict the sound levels at the other the rms errors between predicted and measured maximum received sound exposure levels were less than 5 dB re 1 $\mu Pa^2.s$.

The lack of accurate bathymetry for the Gellibrand Wharf site may explain the larger discrepancies between predicted and measured levels that occurred at that site.

The results presented here apply to a single type of pile at only two locations. It would be extremely useful to extend this work to a greater variety of piles, pile driving equipment, locations and seabed types, thereby building up a library of equivalent source spectra.

ACKNOWLEDGEMENT

Financial and logistical support for data collection and preliminary analysis were provided by the Port of Melbourne Corporation. Malcom Perry and Frank Thomas assisted in field data collection.

REFERENCES

1 David, J. A., "Likely sensitivity of bottlenose dolphins to pile-driving noise", *Water and Environment Journal*, **20**, 48-54 (2006).
2 Popper A.N., Hastings M.C. "The effects of anthropogenic sources of sound on fishes", *Journal of Fish Biology* **75**, 455–489 (2009)
3 Holdgate, G. R., Geurin, B., Wallace, M. W. and Gallagher, S. J. "Marine geology of Port Phillip, Victoria", *Australian Journal of Earth Sciences*, **48** (3), 439 — 455 (2001).
4 Jensen, F. B., Kuperman, W. A., Porter, M. B., Schmidt, H., *Computational Ocean Acoustics*, Springer-Verlag, N.Y., 2000, ISBN 1-56396-209-8.